Instrument Science Report WFC3-2004-05

WFC3 Science Calibration

UVIS Throughput, as measured in the December 2003/January 2004 science verification/calibration campaign

18 April, 2004

by

I. Neill Reid, T. Brown, S. Baggett & G. Hartig, STScI

ABSTRACT

We have completed the first set of science calibration tests of the UVIS channel of Wide-Field Camera 3. This document summarises the results of tests designed to measure the throughput, including data for the majority of the broad- and medium-band filters. We also present wavelength-dependent measurements of four filters (F218W, F225W, F300X and F606W) and the overall system throughput, including the pickoff mirror, camera optics and detector. The measured throughput is 20% higher than predicted at $\lambda<270$ nm, 3-5% lower at 280 – 350 nm and within 2% of expectation at $\lambda>350$ nm.

1 Introduction

Wide-Field Camera 3 (WFC3) is designed to replace Wide-Field Planetary Camera 2 (WFPC2) during servicing mission 4 (SM4) to the Hubble Space Telescope (HST). WFC3 is in the final stages of assembly at Goddard Space Flight Center (GSFC). By late December 2003, the Flight #1 detector had been installed in the UVIS channel together with the control electronics and most ancillary mechanisms, with the exception of the

internal calibration sources. These mechanisms, including the camera, could be controlled using the Science Instrument Test System (SITS), providing the first opportunity to obtain full-system data to verify the system performance for scientific purposes. In consequence, a test calibration campaign was undertaken in December 2003/January 2004. Since all test measurements were obtained under ambient conditions, the detector could not be cooled to the nominal operating temperature of –83 ^{o}C, reaching only –74 ^{o}C. These test data are therefore unsuitable for deriving final calibration measurements.

Initially, the intention was to carry out the series of tests documented in the Wide-Field Camera 3 Mini-Calibration Campaign (MiniCal – seeWFC3 ISR 2003-12). However, alignment tests have shown that the detector is both offset by ~1 millimetre and tilted by x^{o} with respect to the desired location in the flight package. The detector will need to be re-aligned. As a result only a subset of the Mini-calibration tests were undertaken during this campaign. Nonetheless, the data obtained shed interesting light on system performance.

The scientific results from the tests carried out during the December '03/January '04 Mini-Calibration campaign are discussed in a series of WFC3 SIPT Instrument Science Reports. This report summarises the results from a series of tests designed to measure the throughput. In addition to measurements at the central wavelength of most broad- and medium-band filters, we also present analysis of narrow-band data taken with no filter present in the Selectable Optical Filter Assembly (SOFA). Those data provide a measurement of the system throughput (pickoff mirror, optical surfaces in the camera, detector window and detector QE). In both cases, the observed results are compared with predictions derived from models of the properties of the individual components.

2 Test Procedures and Results

The science calibration measurements described here were obtained in mid-December 2003 and early January 2004. WFC3 was mounted on the Radial Instrument Alignment Facility (RIAF) in the Spacecraft Systems Development and Integration Facility (SSDIF) at Goddard Space Flight Center (GSFC). The instrument was mated with the CASTLE Optical Stimulus, which provides flat field, point source and extended targets. The principal light sources for the present set of measurements were xenon and tungsten lamps, fed through a double monochromator and 200-micron fibres to give a 26-pixel diameter image on the WFC3 CCDs. The CASTLE optics mimic the HST OTA, and the image of the extended target can be placed at any location on the detector using steering mirrors, maintaining an appropriate optical path.

The illuminating flux is calibrated by moving the extended target onto either a photomultiplier tube ($\lambda < 300$ nm; Greeley, 2003) or a silicon photodiode (Greeley, 2002). In the latter case, a rotating sector is used to intercept the beam and produce an alternating current. Under normal operations, the sector is not operational when the extended target is illuminating WFC3, but, as discussed by Reid (2004), rotation

continued, reducing the incident flux and the apparent throughput. We have applied the appropriate corrections to the relevant measurements.

WFC3 is controlled via the Science Instrument Test System (SITS), with the instrumental configuration (channel, filter, exposure time, gain, etc) defined either through real-time commanding or using a Science Mission Specification (SMS) procedure. All tests described in this ISR used SMS commanding, based on spreadsheets produced by a dedicated excel tool. The appropriate CASTLE configurations were defined using stimulus control scripts, generated in parallel with the SMS spreadsheets. Further details of the command structure are given in Reid (2004).

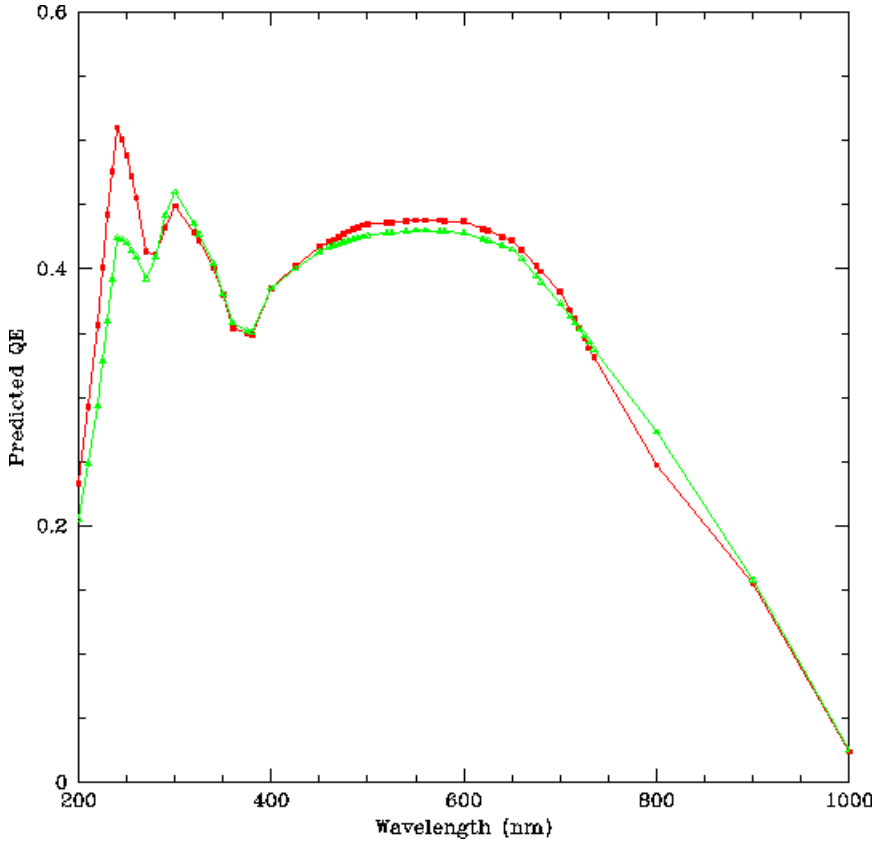

Figure 1 Expected throughput for the two Marconi CCDs installed in the UVIS camera. Chip 1 (CCD c178) is plotted in green; chip 2 (CCD c018) in red. These data are derived using the GSFC Detector Characterization Laboratory (DCL) measurements of CCD quantum efficiency and the predicted throughput of the WFC3 UVIS optical components (excluding photometric or spectroscopic filters).

The tests completed during the MiniCal fall under two headings:

1. Pairs of narrowband measurements made at the central wavelength of broad and medium-band filters
2. For a limited number of filters, narrowband data over a range of wavelengths, allowing determination of the throughput profile of the particular filter. These measurements were interspersed with system throughput measurements.

Test measurements were made with the extended target centred on one of the following alignment positions:

- UV12 at Flight Software co-ordinates (x=279, y=3783) on chip 1 (CCD c178), data read out through Amp B
- UV15 at (x=2972, y=1096) on chip 2 (CCD c018), data read out through Amp C
- UV16 at (x=1198, y=1088) on chip 1 (CCD c178), data read out through Amp A

Chip 2 (CCD c018) has higher quantum efficiency at UV wavelengths (Reid et al, 2003), leading to higher predicted throughput at those wavelengths (Figure 1).

We emphasise that none of the throughput values listed below are based on more than two measurements, and many rely on only a single datum. Repeat measurements generally agree to better than 0.5%, but typical absolute uncertainties are 1-2%. Occasionally, individual datapoints can have significantly higher errors.

2.1 Broad- and Medium-band filters

These measurements were made on 11 December 2003 using SMS VE03S01, described in procedure Verif03 (Reid, 2004). The CASTLE monochromator was used in double mode to give a bandpass of 13 nm, with the wavelength tuned to match the central wavelength of each filter. Two measurements were taken through each filter, with these measurements calibrated independently using either the PMT or Si photodiode, as appropriate. In every case, the two flux calibrations, measured as photons/second incident on the pickoff mirror, agree to better than 0.2%.

Data were taken at position UV16 (CCD c178). Individual throughputs were determined by aperture photometry of the resultant circular images, with the background level determined within a surrounding annulus. The resulting total counts were converted to electrons by multiplying by the appropriate gain (formally 1.5 for these measurements), and the throughput determined by taking the ratio with respect to the incident photons. The raw measurements formally require correction for overcounting at ultraviolet wavelengths (λ<339.68 nm, the critical wavelength), where photons are sufficiently energetic that there is a finite probability of generating two electrons. The correction factor is approximated as $C = \lambda/339.68$, with λ in nm.

In most cases, the two measurements of each filter agree to better than 0.5%; the exception is F625W, where the first measurement gives a throughput only 60% of the second measurement. Nothing unusual was noted at the time and the logged parameters reveal no obvious source of error, but it seems likely that there may have been a delay in configuring the stimulus, and the second (higher) value is listed in Table 1. We also note that measurements were also made of the F475W and F850LP filters; in both cases, the data were overexposed, leading to saturated images. These measurements were not repeated. Allowing for potential systematic errors, the typical uncertainty associated with the measured throughput is ~1%.

Table 1: Throughput: broad and medium-band filters

Filter	λ (nm)/source	Predicted (%)	Measured (%)	Corrected (%)
F218W	218 / Xenon	10.1	10.1	6.5
F225W	225 / Xenon	9.5	19.7	13.1
F275W	275/ Xenon	12.3	10.0	8.1
F336W	336 / Xenon	30.6	24.7	24.4
F390W	390 / Xenon	35.0	31.7	
F438W	438 / Xenon	33.0	32.6	
F555W	555 / Tungsten	37.5	38.3	
F606W	606 / Tungsten	40.3	38.5	
F625W	625 / Tungsten	37.8	39.0	
F775W	775 / Tungsten	24.7	30.2	
F814W	814 / Tungsten	24.3	24.2	
F390M	390 / Xenon	32.3	26.1	
F410M	410 / Xenon	25.8	21.8	
F467M	467 / Xenon	33.2	30.7	
F547M	547 / Xenon	35.7	33.9	
F621M	621 / Tungsten	36.8	38.8	
F689M	689 / Tungsten	34.6	35.8	
F763M	763 / Tungsten	29.9	28.7	
F845M	845 / Tungsten	20.8	20.0	

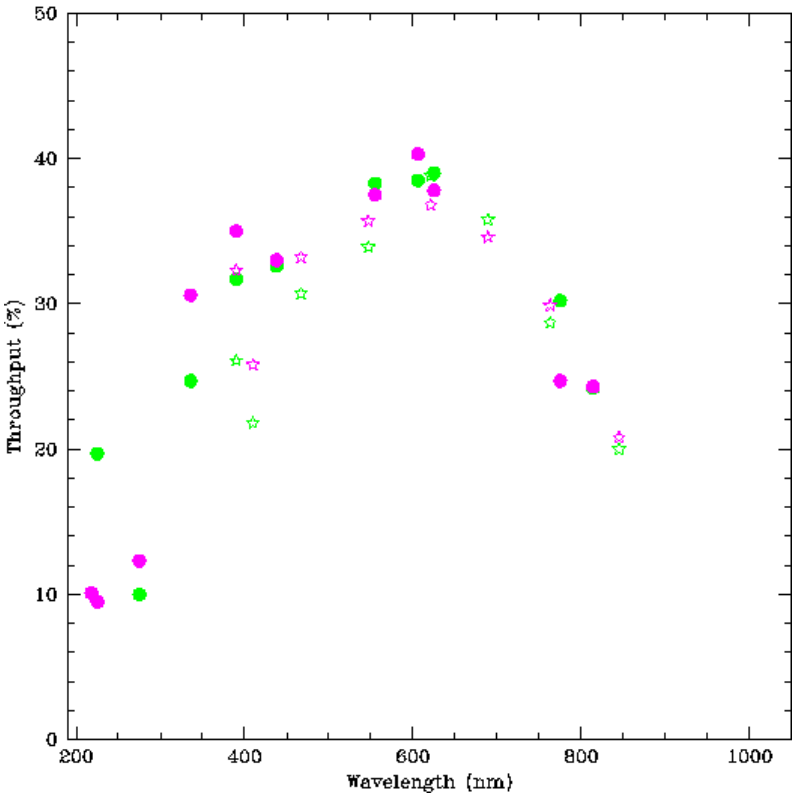

Figure 2: Broad- and medium-band filter throughputs. The predicted values are shown in magenta, the measured values in green, with broadband filters plotted as filled points and medium-band filters as stars. No quantum effect corrections have been made to either predicted or observed values.

Figure 2 and Table 1 show the results from this test procedure. In the table, Column 1 lists the filter; column 2, the central wavelength and light source; column 3, the predicted throughput (from Brown et al, 2003); column 4, the raw value for measured throughput, derived as outlined above; and column 5, the throughput as corrected for quantum effects. As noted above, the latter effects are relevant only for λ<339.68 nm. Given the measuring uncertainties, the observed values are broadly consistent with predictions longward of ~400 nm, fall below the predicted level at 300-400 nm, and exceed predictions at the shortest wavelengths. As discussed further below, these results appear to reflect variations in the system throughput, rather than problems with individual filters.

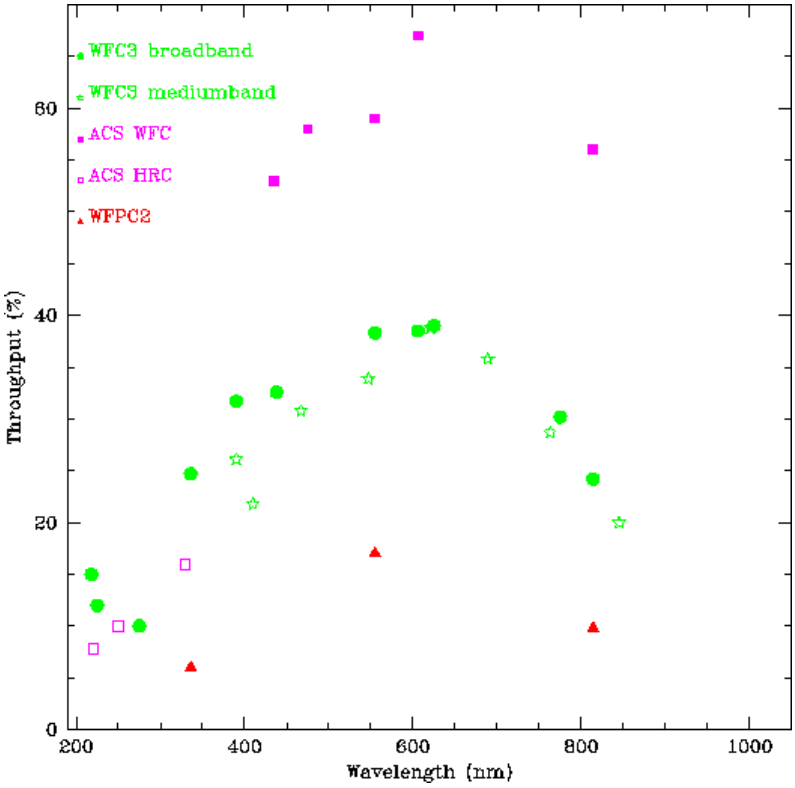

Figure 3: Comparison between the measured throughput of WFC3, ACS and WFPC2. The WFC3 data are taken from Table 1; ACS WFC data are for the F450W, F500, F555W, F606W and F814W filters; ACS HRC data are for F220W, F250W and F350W filters; and WFPC2 data are for the F336W, F555W and F814W filters.

Figure 3 compares the empirical results for WFC3 against on-orbit measurements of throughput for the current optical imaging instruments on HST, Wide-Field Planetary Camera 2 and the Advanced Camera for Surveys. WFC3 has a significantly higher throughput than WFPC2 at all wavelengths. The Wide Field Camera (WFC) on ACS has a significantly higher throughput over most of the wavelength range covered (450-850

nm), reflecting the quantum efficiency of the CCDs, which are optimised for those wavelengths and have minimal response shortward of 450 nm. WFC3 has equal or higher throughput than the ACS High Resolution Camera, and provides a factor of ten improvement in areal coverage.

2.2 The F218W filter

The F218W filter installed in the SOFA is an air-gap filter. The original set of throughput measurements, made on 16 December 2003 via verification script VE09S04, was designed to check for potential degradation in the filter transmission profile, as discussed in procedure Verif09. The extended target was centred on alignment location UV12 (CCD c178) and measurements cover wavelengths between 200 and 275 nm, with bandwidth 4 nm.

While the test was not fully successful, the results revealed the presence of significant wavelength dependence in the relative strength of the prominent ghosts present in this filter (see Brown & Lupie, 2004, for a full discussion). As a consequence, a revised version of this test (VE09S09) was completed on January 13, with the extended target centred on UV15 (CCD c018) and covering wavelengths from 200 to 325 nm. Measurements through F218W were bracketed by measurements through CLEAR (i.e. no filter in the SOFA – we shall refer to these measurements as the `system throughput'.)

A further set of throughput measurements was made on 13 January 2004 via SMS VE09S10, sampling the throughput at wavelengths of 275 to 1000 nm. Coupled with data taken in the F225W filter, these measurements were made at location UV15 (CCD c018) at bandwidth 5 nm.

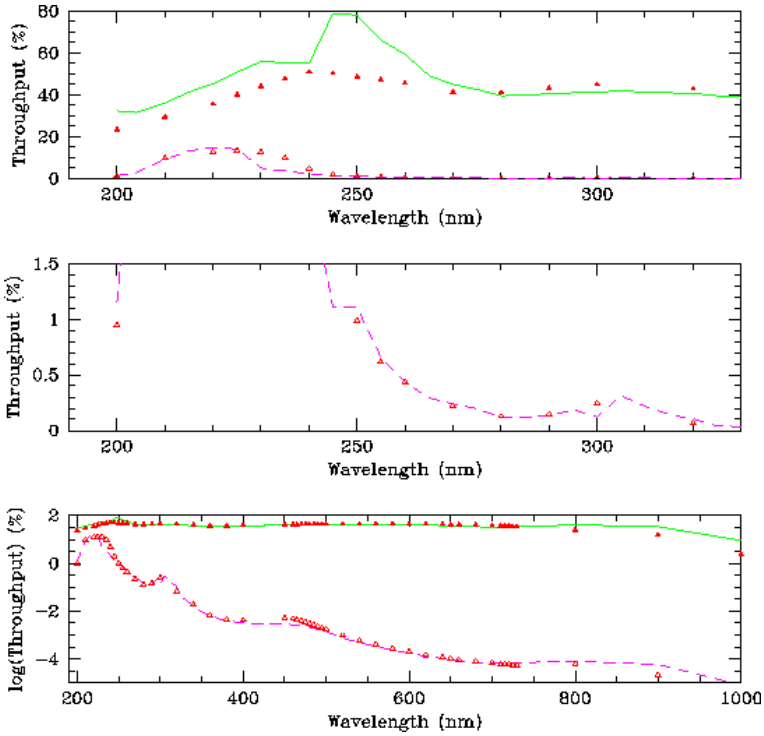

Figure 4: Measured and predicted throughputs for the F218W filter. The green solid line gives the measured system throughput (i.e. with no filter in the SOFA), the magenta dashed line plots the filter data and the red triangles mark the predicted values.

Results from VE09S09 and VE09S10 are listed in Table 2 and illustrated in Figure 4. Note that the data plotted are not corrected for double counting at short wavelengths; corrected values at the relevant wavelengths are given in Table 2. In a few cases, the system throughput values are interpolated from other measurements (see section 2.4) – those data are identified by an asterisk. The main conclusions that we draw from this comparison are as follows:

1. The measured system throughput is significantly higher than predicted at wavelengths between 200 and 275 nm. The extremely high throughput values at 245-260 nm are not confirmed by F300X measurements (see 2.4).
2. The overall shape of the red wing of the filter is close to predictions, including the secondary peak at ~300 nm.
3. The transmission falls below 10^{-4} (0.01%) longward of 325 nm, consistent with the CEI specification, and leading to minimal red leak problems.

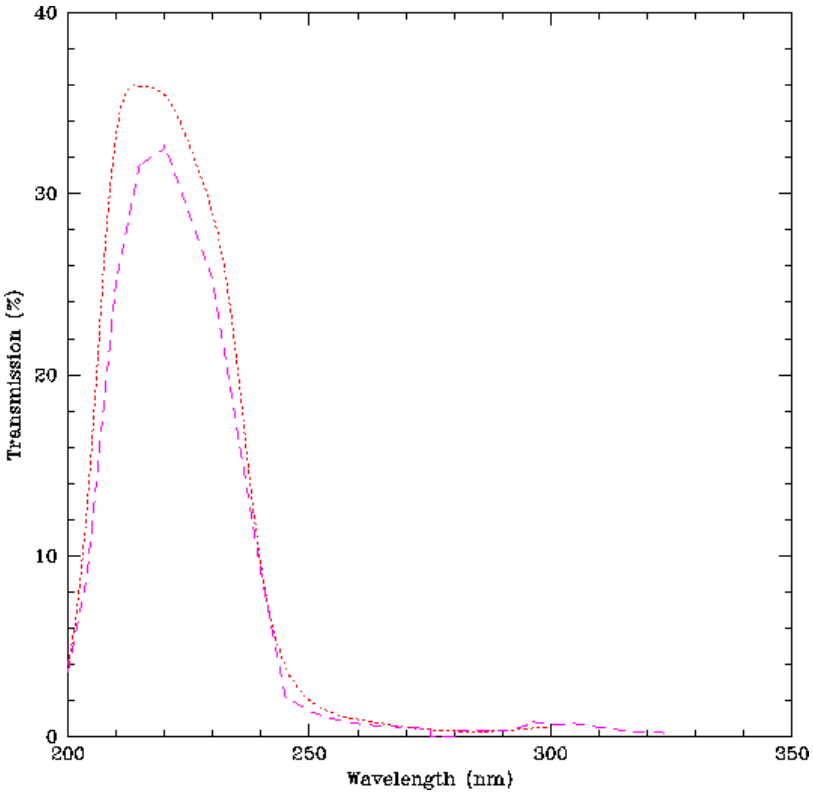

Figure 5: Transmission curve of the F218W filter. The dashed line shows the values deduced from our measurements, while the dotted line plots measurements of the transmission before installation in the SOFA

Table 2: F218W throughput measurements, 200-325 nm, VE09S09/10

λ (nm)	F218W – pred (%)	Obs (%)	Corr (%)	CLEAR – pred (%)	Obs (%)	Corr (%)
200	0.95	1.15	0.678	23.3	32.3	19.0
204	3.82	2.84	1.70	25.0	32.1	18.9
210	9.75	9.10	5.62	29.4	37.3	22.4
215	11.2	13.1	8.28	33.0	42.2	26.1
220	12.6	14.8	9.57	35.6	46.1	29.4
225	13.2	14.1	9.33	40.1	50.8	33.7
230	12.8	4.95	3.35	47.6	57.4	37.8
240	4.80	2.24	1.57	51.1	56.0	38.7
245	1.98	1.10	0.796	50.1	89.8	56.9
250	0.99	1.10	0.812	48.8	81.8	57.4
255	0.62	0.66	0.494	47.2	67.2	49.7
260	0.44	0.43	0.333	45.5	62.7	45.3
265	0.33	0.29	0.229	43.2	50.5	38.3
270	0.22	0.24	0.190	41.3	47.3	35.8
275	0.17	0.20	0.159	41.2	42.4	34.4
280	0.13	0.12	0.097	41.1	39.5	32.5
285	0.14	0.12	0.102	42.1	40.4	33.3
290	0.15	0.13	0.113	43.2	40.7	34.5
295	0.20	0.19	0.164	44.1	42.0	35.6
300	0.25	0.12	0.108	44.9	41.9	36.4
305	0.23	0.31	0.279	45.4	42.6	37.6
310	0.16	0.22	0.200	44.8	42.4	37.7
315	0.10	0.14	0.132	44.1	41.6	38.0
320	0.068	0.10	0.0975	42.8	41.5	38.2
325	0.048	0.041	0.0395	42.2	40.3	37.8
VE09S10						
350	0.0105	9.27×10^{-3}		38.0	36.3*	
375	5.03×10^{-3}	4.08×10^{-3}		35.0	34.9*	
400	4.21×10^{-3}	3.18×10^{-3}		38.5	38.6	
425	4.47×10^{-3}	2.89×10^{-3}		40.2	39.5*	
450	4.99×10^{-3}	2.92×10^{-3}		41.7	40.5	
475	3.52×10^{-3}	2.34×10^{-3}		42.7	41.2*	
500	1.66×10^{-3}	1.38×10^{-3}		43.5	41.9	
525	8.36×10^{-4}	6.67×10^{-4}		43.6	42.0*	
550	4.80×10^{-4}	3.98×10^{-4}		43.8	41.8	
575	2.95×10^{-4}	2.47×10^{-4}		43.8	42.0*	
600	1.93×10^{-4}	1.68×10^{-4}		43.7	42.2	
625	1.34×10^{-4}	1.21×10^{-4}		43.0	42.5*	
650	1.01×10^{-5}	9.17×10^{-5}		42.2	42.1	
675	7.76×10^{-5}	7.33×10^{-5}		40.2	40.0*	
700	6.43×10^{-5}	6.69×10^{-5}		38.2	37.6	

800	7.05×10^{-5}	7.72×10^{-5}		24.7	20.3	
900	2.17×10^{-5}	5.85×10^{-5}		15.5	16.7	
1000	2.42×10^{-6}	8.20×10^{-6}		2.4	4.5	

We can measure the transmission curve for the F218W filter by taking the ratio between the observed throughputs with the filter in place and with the SOFA set to CLEAR (columns 3 and 6 in Table 1). Figure 5 plots the results of this exercise, comparing the empirical throughput against measurements made prior to the filter being installed in the SOFA (data taken from http://wfc3.gsfc.nasa.gov/private/soc/filters/uvis_filt_trans_data.html). The agreement is reasonable, although the peak transmission is lower than the predicted value by 3-4%.

2.3 The F225W Filter

The F225W filter also has an air-gap design and exhibits prominent ghosting (Brown & Lupie, 2004). Narrowband throughput measurements covering wavelengths between 200 and 275 nm at 4 nm bandwidth were made on December 17 2003, via SMS VE09S05 (UV12 – CCD c178). Those measurements were supplemented by longer wavelength data (275-1000 nm, 5 nm bandwidth) taken on 13 January 2004 via SMS VE09S10, as described in the previous section. The results are illustrated in Figure 6 and listed in Table 3.

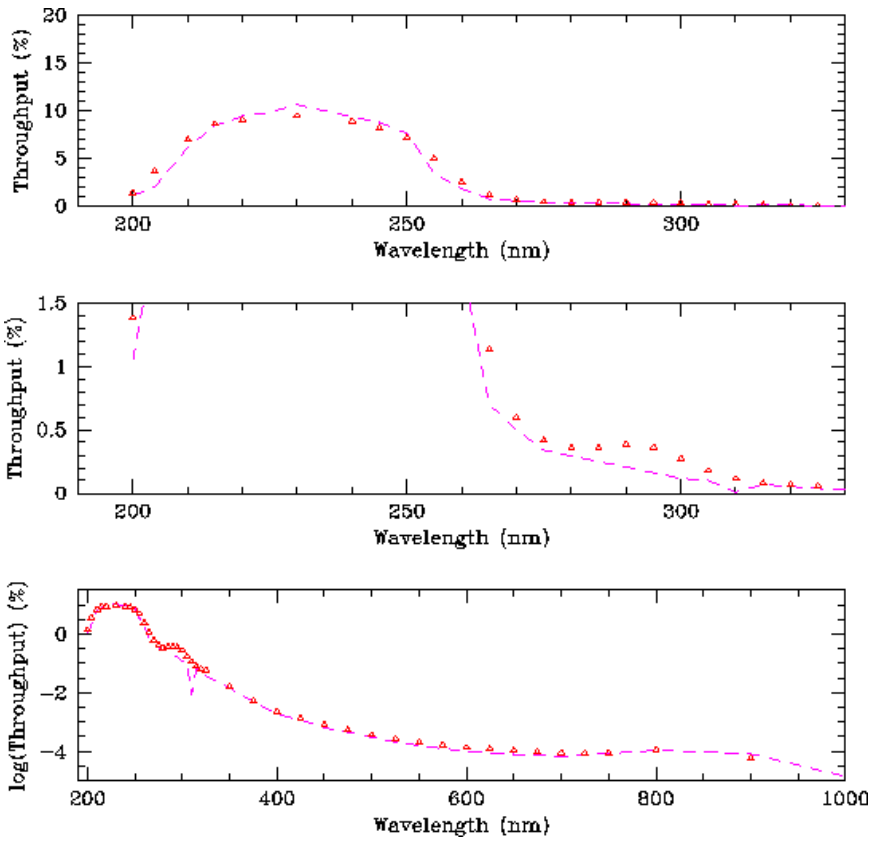

Figure 6: Throughput measurements for F225W. The dashed line marks empirical measurements of the filter throughput, while the open triangles plot the expected values.

The main results from this comparison can be summarized as follows:

1. The measured throughput for F225W between 200 and 240 nm is consistent with predictions.
2. The red wing of the filter does not appear to show the expected plateau between 280 and 300 nm, although note that measurements are limited to 275 and 300 nm.
3. As with F218W, throughput falls below 0.01% at ~350 nm, with consequently low red leak. Note that the measured profile shows the slight predicted upturn in throughput at 800 nm.

Table 3: F225W throughput data

λ (nm)	**F225W – pred (%)**	**Obs (%)**	**Corr (%)**
200	1.38	1.05	0.618
204	3.65	2.00	1.20
210	6.95	6.10	3.77
215	8.59	8.41	5.32
220	9.04	9.42	6.09
230	9.42	10.6	7.17
240	8.89	9.33	6.57
245	8.15	8.68	6.27
250	7.15	7.61	5.57
255	4.94	3.39	2.55
260	2.49	1.79	1.38
265	1.13	0.700	0.546
270	0.600	0.495	0.396
275	0.418	0.337	0.273
VE09S10			
300	0.278	0.117	0.103
325	0.0607	0.0381	0.0365
350	0.0160	0.0149	
375	5.23×10^{-3}	5.11×10^{-3}	
400	2.31×10^{-3}	1.89×10^{-3}	
425	1.37×10^{-3}	1.19×10^{-3}	
450	8.19×10^{-4}	6.43×10^{-4}	
475	5.45×10^{-4}	4.63×10^{-4}	
500	3.74×10^{-4}	3.00×10^{-4}	
525	2.75×10^{-4}	2.11×10^{-4}	
550	2.17×10^{-4}	1.62×10^{-4}	
575	1.69×10^{-4}	1.26×10^{-4}	
600	1.39×10^{-4}	9.85×10^{-5}	
625	1.21×10^{-4}	8.82×10^{-5}	
650	1.10×10^{-4}	8.00×10^{-5}	
675	9.92×10^{-5}	7.92×10^{-5}	
700	9.27×10^{-5}	6.77×10^{-5}	
800	1.19×10^{-4}	1.08×10^{-3}	
900	5.92×10^{-5}	8.37×10^{-5}	

1000	7.68×10^{-6}	1.44×10^{-5}	

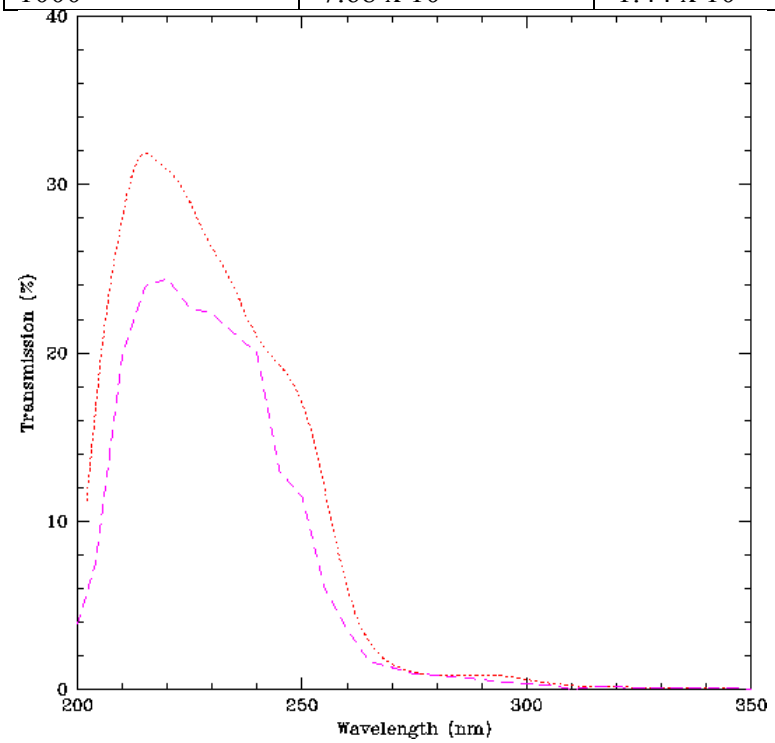

Figure 7: Filter transmission for F225W - as in Figure 4, the dashed line plots our measurements and the dotted line oulines the pre-installation data.

As with F218W, we can determine the filter transmission profile by taking the ratio between the F225W and CLEAR throughput data. The results are plotted in Figure 7. These results indicate a narrower passband, with the peak throughput approximately 20% lower than expected.

2.4 The F300X Filter

The F300X filter used in these tests is also an air-gap filter and, like F218W and F225W, exhibits ghosting, although the brightest ghosts are ten times less prominent than in the two shorter-wavelength ultraviolet filters (see Brown & Lupie, 2004, for further details). Given the strong wavelength dependence in the relative brightness of the ghosts noted for both F218W and F225W, an extensive series of narrowband throughput measurements were also undertaken for the F300X filter. Those measurements were made via SMS VE09S13, which covered wavelengths between 200 nm and 1000 nm (bandwidth 5 nm), bracketing the F300X measurements with CLEAR system throughput measurements.

The SMS was started on 16 January 2004, with data taken covering wavelengths 200-700 nm. Administrative issues caused the SMS to be interrupted at that point, and the final datapoints (800-1000 nm) were obtained on 20 January 2004. All measurements were made at alignment location UV15 (CCD c018). The resulting throughput measurements are illustrated in Figure 8 and listed in Table 3.

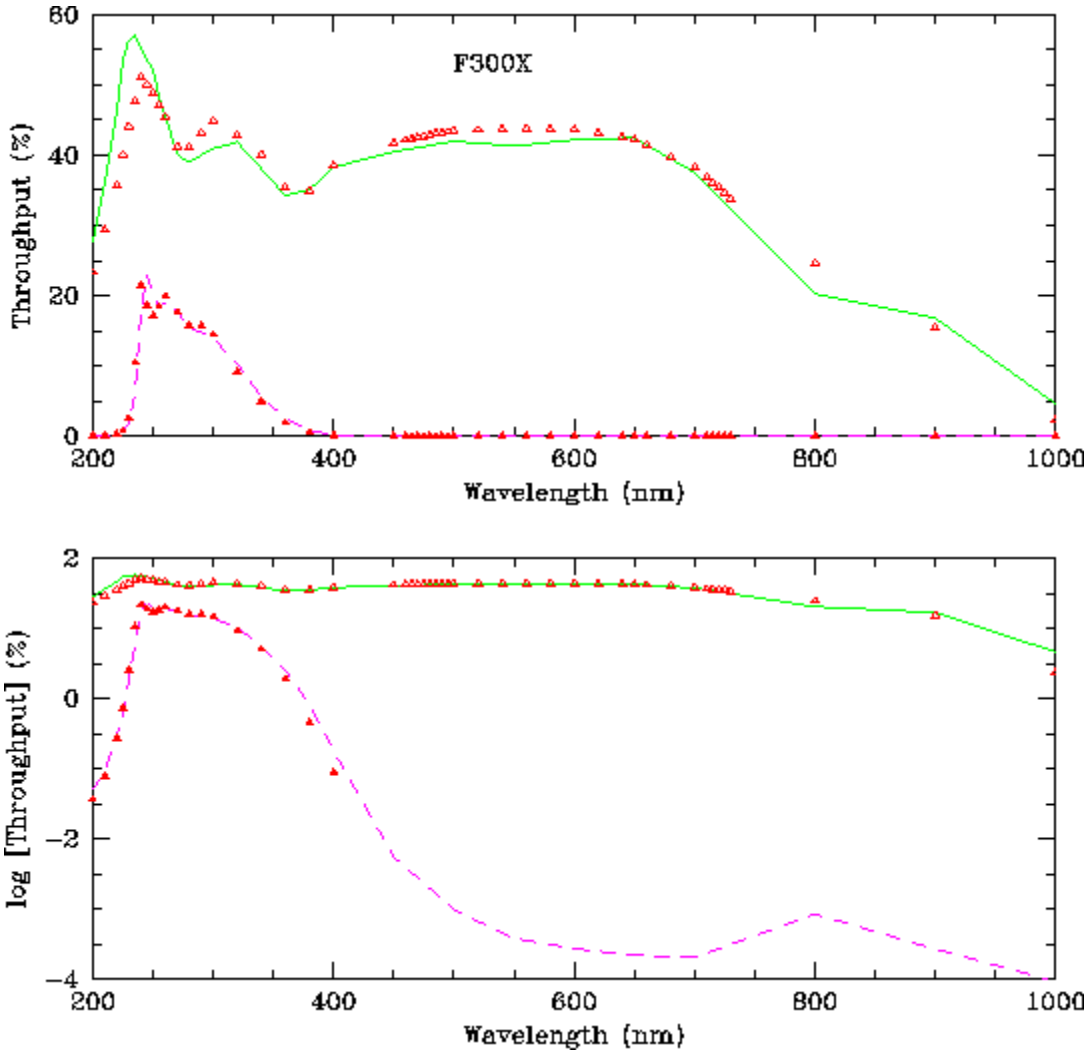

Figure 8: Throughput measurements for F300X. As in Figures 3 and 5, the filter throughput data are plotted as a dashed line, while the system throughput (CLEAR) is shown as a solid line. Solid and open triangles mark the predicted throughput values for the system and filter, respectively.

The main conclusions we draw from this comparison are as follows:

1. The high system throughput shortward of 270 nm derived from procedure VE09S05 is confirmed by these independent data, although these measurements do not reach the (rather implausible) peak of 80%+ at 245-260 nm. The current dataset is likely to be more reliable, since it was obtained later in the calibration campaign when both the system and the operators were more experienced.
2. The system throughput falls below predictions by 3-5% between 270 and 370 nm, but closely matches expectations at longer wavelengths.
3. The F300X throughput is broadly consistent with predictions, falling below 0.01% longward of 425 nm.

Table 4: F300X throughput data

λ (nm)	F300X – pred (%)	Obs (%)	Corr (%)	CLEAR – pred (%)	Obs (%)	Corr (%)
200	0.037	0.0497	0.0299	23.3	27.8	16.4
210	0.076	0.0906	0.0560	29.3	35.9	22.2
220	0.27	0.291	0.189	35.6	46.3	29.9
225	0.73	0.634	0.420	40.1	53.9	35.7
230	2.53	1.81	1.23	44.2	56.2	37.6
235	10.5	5.91	4.09	47.6	57.0	40.1
240	21.5	18.3	12.9	51.1	55.9	41.5
245	18.6	22.8	16.5	48.8	53.5	39.4
250	17.2	20.1	14.8	47.2	52.0	41.4
255	18.4	18.4	13.8	46.2	48.3	38.3
260	20.0	19.0	14.5	45.5	45.7	39.7
270	17.6	17.9	14.2	41.3	40.1	34.1
280	15.8	15.3	12.6	41.1	39.7	31.0
290	15.7	14.7	12.6	43.2	41.3	32.3
300	14.4	13.9	12.3	44.9	42.0	36.1
320	9.2	10.3	9.66	42.8	42.4	38.9
340	5.0	5.61		40.1	39.5	
360	1.9	2.51		35.4	35.2	
380	0.5	0.805		35.1	35.1	
400	0.088	0.178		38.5	38.6	
450		5.56×10^{-3}		41.7	41.5	
500		9.75×10^{-4}		43.5	41.9	
550		3.80×10^{-4}		42.8	42.8	
600		2.75×10^{-4}		43.5	42.3	
650		2.20×10^{-4}		43.7	42.3	
700		2.05×10^{-4}		38.3	37.5	
800		8.53×10^{-4}		24.7	20.2	
900		2.69×10^{-4}		15.5	16.7	
1000		9.40×10^{-5}		2.37	4.6	

Again, we can determine the transmission profile for the F300X filter by taking the ratio between the throughput measured with that filter in place and the system throughput measurements at the same wavelength. The results are shows in Figure 9. The overall shape of the profile and the transmission values are close to expectations, but the data suggest a systematic shift of +5 nm. Thus, the narrow peak expected at 240 nm is measured as being at 245 nm. This offset is comparable to the bandwidth of the incident monochromator flux, but we do not see evidence for similar shifts in the other filter profiles measured using this technique. While no apparent performance anomalies were noted, either during the test or in subsequent checking, it is possible that the wavelengths listed in the data headers are out of step with the actual measurements.

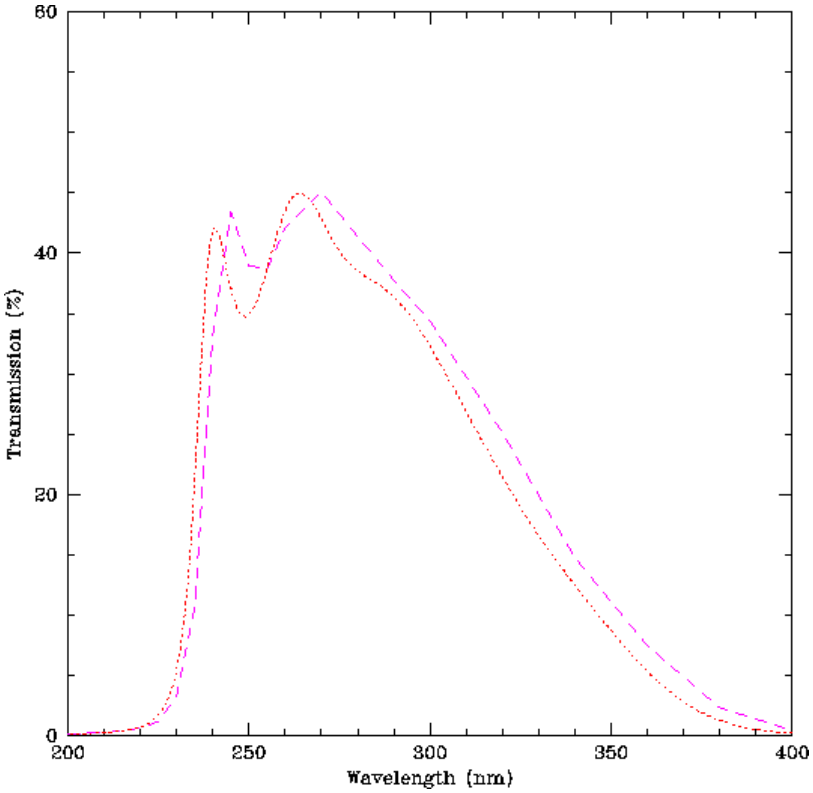

Figure 9: Transmission profile for f300X filter. As in previous figures, the dashed line plots the empirical results, and the dotted line the expected profile, based on pre-installation measurement.

2.5 The F606W Filter

The final filter subjected to detailed scrutiny in the Dec'03/Jan'04 MiniCal is the F606W filter. This is not an air-gap design, but point sources exhibit a series of `spot' ghosts that closely mimic the spatial profiles of unresolved sources (see Brown & Lupie, 2004). As a consequence, a series of narrowband measurements were made to determine the relative intensity of those ghost images as a function of wavelength. The measurements were made via SMS VE09S11 on 14 January 2004. The extended target was centred at location UV15 (CCD c018), and 4 nm bandwidth data taken at wavelengths from 460 to 735 nm.

The results of these measurements are listed in Table 5 and presented in Figure 10. As before, we have compared the empirical throughput estimates against predictions from Brown et al's (2003) model. There is good agreement. The most significant discrepancy lies at 500 nm, where the measured value, 24.7%, falls ~10% below expectation. Since the 500 nm datum is based on a single measurement, and the adjacent empirical values are 32.4% (495 nm) and 34.8% (520 nm), it is likely that this offset is due to measuring error. The overall throughput is ~1% below the expected values between 540 and 580 nm, while the red wing of the observed passband is truncated more sharply (at 695-715 nm) than predicted by the model.

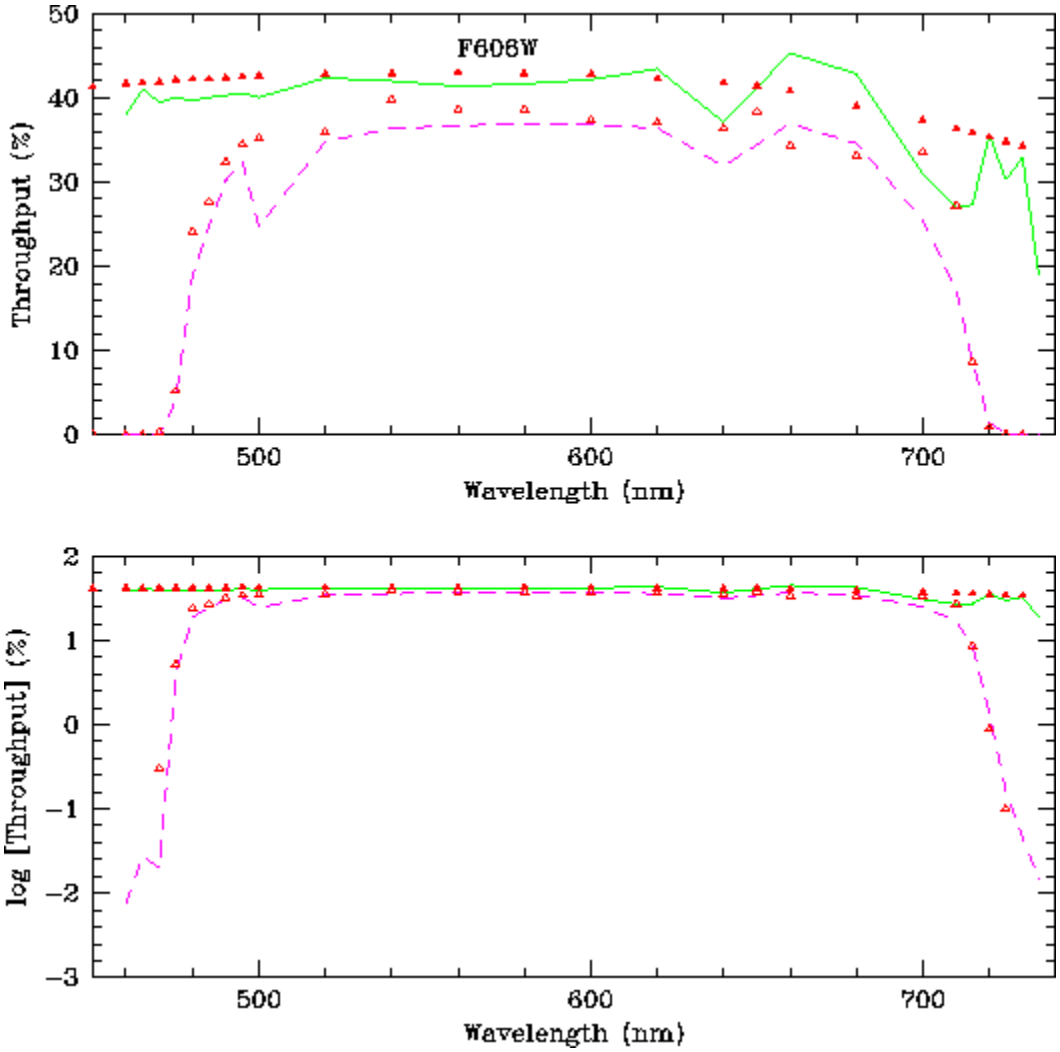

Figure 10: Throughput measurements for the F606W filter. As in previous figures, filter throughput data are plotted as a dashed line, while the system throughput (CLEAR) is shown as a solid line. Solid and open triangles mark the predicted throughput values for the system and filter, respectively.

λ (nm)	F606W – pred(%)	Obs (%)	Clear – Pred(%)	Obs (%)
460	0.0034	0.00753	42.1	39.3
465	0.032	0.0269	42.4	41.9
470	0.34	0.0202	42.5	40.9
475	5.2	4.06	42.7	40.6
480	24.6	19.02	42.9	40.8
485	28.2	24.65	43.1	41.1
490	33.0	30.2	43.3	41.4
495	35.2	32.4	43.4	41.7
500	35.9	24.7:	43.5	41.3
520	36.7	34.8	43.6	43.2
540	40.7	36.4	43.7	43.0

560	39.4	36.7	43.8	42.5
580	39.4	39.9	43.7	42.5
600	38.2	36.8	43.7	43.7
620	37.8	36.4	43.1	43.4
640	37.0	31.9	42.6	37.1
660	35.1	36.9	41.5	45.3
680	34.0	34.6	39.8	42.8
700	34.5	25.5	38.3	30.9
710	27.6	17.2	36.8	27.0
715	8.8	8.64	36.1	27.3
720	0.93	1.37	35.4	35.7
725	0.12	0.163	34.6	30.3
730	0.023	0.0463	33.9	33.0
735		0.0147		18.9

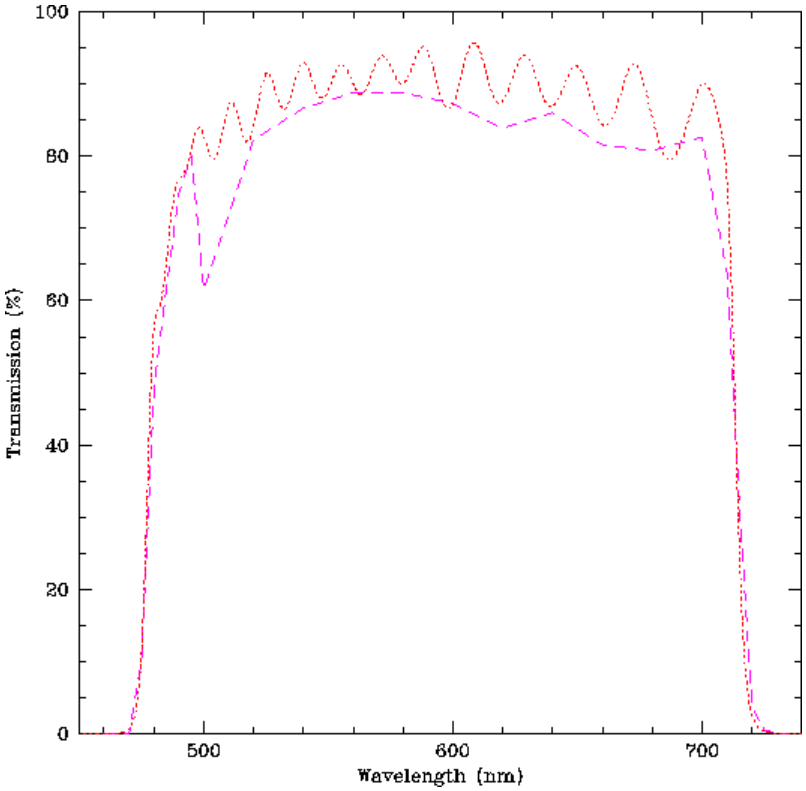

Figure 11: Comparison between the expected (dotted line) and measured (dashed line) transmission profiles of the F606W filter.

The pre-installation measurement of the F606W filter shows extensive fine-scale structure between 500 and 700 nm – i.e. over the full range of maximum throughput. Our measurements were made with a bandwidth of 4 nm, comparable to, or even exceeding, the expected variations. As a result, it is not surprising that the predicted fine-scale variations are not detected (Figure 11). Setting aside the apparent dip at 500 nm

(discussed above), the measured transmission values are ~3-5% lower than expected, based on the pre-installation filter scans.

3 Summary and Conclusions

We have presented an empirical analysis of the throughput of the WFC3 UVIS channel. The data discussed in this report were obtained as part of the MiniCalibration campaign undertaken in December 2003 and January 2004, and consist of measured throughput at the central wavelength of most broad- and medium-band filters, together with detailed throughput profiles for the UVIS system (unfiltered) and the F218W, F225W, F300X and F606W filters. The main results are as follows:

1. The system throughput is significantly higher than expected at the shortest wavelengths, from 200-270. Setting aside the anomalously high measurements at 245-260 nm from VE09S05, the excess is ~20%. This offset is within the uncertainties of the initial GSFC DCL quantum efficiency measurements.
2. The system throughput is 3-5% lower than expected between 280 and 370 nm, with the maximum difference at 300 nm where the measured value is 41%, rather than the predicted 46%.
3. The system throughput between 380 and 1000 nm is within 2% of the predicted values – consistent, within the measuring uncertainties.
4. The measured throughputs for the broad- and medium-band filters are broadly consistent with expectation. The main exceptions are filters falling in the 270-400 nm range, which have lower throughput than expected, and the F218W and F225W filters, which have higher throughput than expected. These discrepancies are entirely consistent with the differences between the predicted and measured system throughput.
5. The throughput profile measured for the F218W filter is generally consistent with the predicted shape, although the peak value is lower by ~3%.
6. The throughput profile measured for the F225W filter is also consistent in shape with predictions, but has lower values over the full wavelength range.
7. The F300X filter profile appears shifted to the red by ~5 nm, although the throughput values are broadly consistent with predictions. This may reflect an anomaly in the nominal wavelengths of those measurements.
8. The F606W filter profile is close to expectations, although with a slightly sharper red cutoff than predicted.

All of these conclusions should be considered provisional, given that the detector was not operating under nominal conditions and the restricted size of the calibration dataset.

References

T. Brown, O. Lupie, B. Hilbert, S. Baggett, 2003, ISR WFC3-2003-13, A Throughput Tool for WFC3

T. Brown & O. Lupie, 2004, ISR WFC3-2004-04, Filter ghosts in the WFC3 UVIS channel

B. Greeley, 2002, WFC3-417-BWG-025, CASTLE Silicon Photodiode Flux Calibration

B. Greeley, 2003, WFC3-577-RCT-002, CASTLE PMT Calibration

I. N. Reid, P. Knezek, O. Lupie et al, WFC3-2003-03, WFC3 UVIS CCD flight detectors and operations
I. N. Reid, 2004, ISR WFC3-2004-02, Summary assessment of December 2003/January 2004 science verification/calibration campaign